Catalysis Today 180 (2012) 25–33

Contents lists available at ScienceDirect

Catalysis Today

journal homepage: www.elsevier.com/locate/cattod

The effect of reaction conditions on the apparent deactivation of Ce–Zr mixed oxides for the catalytic wet oxidation of phenol

J.J. Delgado, X. Chen, J.A. Pérez-Omil, J.M. Rodríguez-Izquierdo, M.A. Cauqui*

Departamento de Ciencia de los Materiales e Ingeniería Metalúrgica y Química Inorgánica, Facultad de Ciencias, Universidad de Cádiz, E-11510 Puerto Real (Cádiz), Spain

ARTICLE INFO

Article history:
Received 1 February 2011
Received in revised form 18 March 2011
Accepted 21 March 2011
Available online 1 May 2011

Keywords:
Phenol
Catalytic wet oxidation
Ce–Zr oxides
Carbonaceous deposit
Deactivation
TEM

ABSTRACT

A series of Ce–Zr mixed oxides with different composition have been characterized and used as catalysts in the catalytic wet oxidation (CWO) of phenol. The addition of Zr significantly enhanced the redox and catalytic activity of ceria. However, a catalytic activity drop occurred for zirconium contents higher than 80%, which is related with a ZrO_2 segregation observed in Zr-rich oxides. The effects of the temperature of reaction, the oxygen partial pressure and the phenol/catalyst ratio on the activity for the oxidation of phenol and the selectivity to CO_2 were also investigated. The values for CO_2 selectivities were greatly influenced by the formation of a carbonaceous deposit adsorbed on the catalyst surface. The results indicated that these C-deposits can be totally oxidized by selecting appropriate operating conditions, thus obtaining catalytic systems with a very promising performance for phenol abatement. A mechanism is proposed to interpret the role of the carbonaceous deposits in the oxidation of phenol as a function of the reaction conditions.

1. Introduction

The waste management initiatives have increased in the recent years in response to the dire need of the environmental protection. A clear example of such initiatives is the increasing stringent environmental legislation concerning to the limits of pollutants, which led to the development of new wastewater purification technologies and the improvement of the pre-existing ones. In this sense, the elimination of organic pollutants in wastewaters has been a major issue and intensive research effort has been focused on the development of new technologies for water depuration.

The wet air oxidation (WAO) is one of the most attractive processes for treating wastewaters which are too dilute to incinerate or when biological processes are less effective because of pollutant toxicity [1–4]. Although WAO is currently used in treatment of toxic or refractory substances [5], it requires elevated pressures (0.5–20 MPa) and temperatures (150–325 °C) [3]. However, the use of catalysts (catalytic wet oxidation, CWO) implements this technology thus making the process economically much more attractive [1,6].

Several homogeneous catalysts ($CuSO_4$ and other inorganic salts) exhibit good performances for different wastewater treatments [7,8]. However, the high toxicity of the catalyst ions requires a separation step, such as precipitation, to remove them from the final effluent. This negative aspect can be overcome by using heterogeneous catalysts, which are easily recoverable and reused. Among the heterogeneous catalysts used in CWO, the Ce-based oxides have attracted attention because of their excellent performance, often attributed to their capacity to exchange oxygen with the reaction environment [9]. In particular, the oxides of cerium and manganese have demonstrated an excellent activity in the oxidation of model pollutants, such a phenol [10–12]. However, these systems suffer two types of deactivation mechanisms: (i) the leaching of the active phase and (ii) the formation of carbonaceous deposits. In accordance with the results of the literature, both processes are associated with the presence of manganese [13]. On the other hand, it is well known that the redox properties and thermal stability of pure ceria can be enhanced by adding zirconia (ZrO_2) to form solid solutions of the $Ce_{1-x}Zr_xO_2$ type [14,15,9], thus making of these formulations good candidates for CWO purposes.

In the present work we report on the catalytic performances in phenol oxidation of a series of Ce–Zr mixed oxides with molar contents of Zr from 20 up to 80%. We also include pure ceria for comparison. The close relationship between the redox and nanostructural properties of the oxides and their catalytic performances is discussed. We also investigate the effect of the temperature, oxygen partial pressure and phenol/catalyst ratio on phenol conversion and selectivity to CO_2. The characterization of the used catalysts by means of transmission electron microscopy allowed us to obtain evidences of the formation of carbonaceous deposits on the surface

* Corresponding author. Tel.: +34 956 016333; fax: +34 956 016288.
E-mail address: miguelangel.cauqui@uca.es (M.A. Cauqui).

0920-5861/$ – see front matter © 2011 Elsevier B.V. All rights reserved.
doi:10.1016/j.cattod.2011.03.069

Table 1
Chemical composition (molar content) measured by ICP, and textural properties of fresh catalysts.

Sample	Ce (%)	Zr (%)	S_{BET} ($m^2\ g^{-1}$)	V_{micro} ($cm^3\ g^{-1}$)	Average pore diameter (Å)	D/(nm)[a]
CZ100	100	0	100	0.0020	65	11.0
CZ80	80	20	111	0.0003	40	7.4
CZ68	68	32	100	0.0007	65	8.0
CZ50	58	42	106	0.0018	55	7.5
CZ15	15	85	95	0.0006	95	6.9

[a] Particle size obtained from X-rays analysis of peak (1 1 1).

of the catalytic particles. By using carbon-mass balances calculations, the influence of the operating conditions on the deposit formation process was established.

2. Experimental

High surface mixed oxides with different Ce/Zr molar ratio (15/85, 50/50, 68/32, 80/20 and 100/0) were supplied by Rhodia. They will be hereafter referred to as CZ*X*, where *X* indicates the Ce% molar content (Zr% molar content = 100 − *X*). Table 1 summarizes the results concerning chemical composition, measured by inductively coupled plasma atomic emission spectroscopy (ICP-AES), and textural properties, determined by nitrogen adsorption–desorption isotherms at −196 °C (Micromeritics Asap 2020C). The pore size distribution was obtained by applying the BJH method [16].

The structural characterization of the fresh and used catalysts was obtained by using transmission electron microscopy (TEM) and X-ray diffraction. X-ray diffraction (XRD) analyses were performed on a Philips PW1820 diffractometer (Cu Kα radiation) operating at 40 kV and 40 mA. TEM and energy dispersive spectroscopy (EDS) measurements were performed on a JEOL JEM-2010 microscope with a structural resolution of 0.19 nm.

Temperature-programmed reduction (TPR) and O_2 uptake measurements were carried out following the procedures described in [17].

The used catalysts were also investigated by temperature programmed oxidation (TPO), to obtain the burn-off profiles of the carbonaceous deposits. For TPO experiments, a mixture of 5% O_2 in helium was used as oxidant agent. The gas flow was 60 $cm^3\ min^{-1}$ and the heating rate set to 10 °C min^{-1}. The effluent gas was analyzed by using a mass spectrometer (Sensorlab 200D instrument).

The CWO tests were carried out in a 500-mL autoclave (Autoclave Engineers), operating in batch mode. The reactor was equipped with a pollutant injector, a valve for sampling, a magnetic stirrer and a pressure gauge. The autoclave was initially charged with 250 mL of distilled water and 1 g of catalyst. The vessel was pressurized with a certain pressure of oxygen (2.0 MPa) and heated to the reaction temperature (120–160 °C). Once the desired temperature was reached, a phenol solution was injected into the autoclave under pressure of nitrogen (3.5 MPa), leading to an initial phenol concentration of 650 ppm (500 ppm of carbon). Liquid samples (3 mL) were periodically withdrawn from the reactor and analyzed. Total organic carbon (TOC) was measured by using a Shimadzu TOC analyzer, while phenol and organic intermediates were identified and quantified by gas chromatography (Carlo Erba, GC 8000 TOP Series) using a flame ionization detector and a column made of Nukol™. The liquid was also analyzed by ICP-AES, to investigate the leaching of active phase. The carbon content on the surface of the used catalyst was quantified by CHN elemental analysis (Carlo Erba, model 1106). Blank experiments (without catalyst) were performed under the most severe operation conditions used in this work (T^{o} = 160 °C, P_{O_2} = 2.0 MPa). No activity was observed in these experiments.

3. Results and discussion

3.1. Characterization of the fresh catalysts

Table 1 summarizes the most important results derived from the characterization studies on Ce–Zr oxides. The specific surface areas of all the oxides were quite close in the range from 95 to 110 $m^2\ g^{-1}$. In all the cases, the nitrogen isotherms were of type IV, according to the BDDT classification [16]. The mean particle sizes of the oxides, obtained by X-ray diffraction, were in good agreement with the experimental BET surface areas. All the series presented a quite narrow distribution of pore diameters, the mean diameter varying from 40 to 95 Å. The *t*-plots indicated the absence of significant microporosity, the contribution of V_{micro} remaining below 1%.

The XRD patterns of the Ce–Zr mixed oxides are shown in Fig. 1. For Ce-rich compositions (CZ80, CZ68 and CZ50), these patterns are dominated by sharp and intensive diffraction peaks corresponding to cubic fluorite-type CeO_2 structure (JCPDS 43–1002). According to the phase diagram proposed by Yashima et al. [18,19], a partial

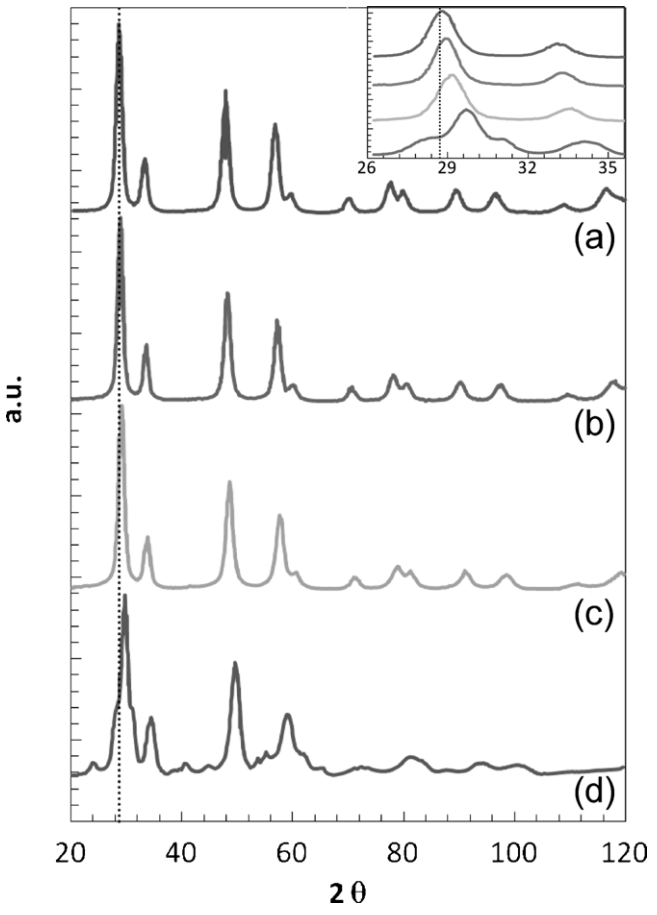

Fig. 1. X-ray diffraction pattern of samples CZ80 (a), CZ68 (b), CZ50 (c) and CZ15 (d).

tetragonalization would be expected in the case of CZ50 sample. However, in our case, it was not possible to clearly identify the double peak (1 1 2)/(2 0 0) of the tetragonal structure, due to the very close position of the theoretical values of these peaks. No other crystalline or amorphous phases were detected in these oxides by XRD, thus assuming that all the Zr cations were incorporated into the CeO_2 lattice forming a CeO_2–ZrO_2 solid solution. The substitution of the larger Ce^{4+} (0.97 Å) by the smaller Zr^{4+} (0.84 Å) was also deduced from a gradual shifting in the position of the ceria (1 1 1) diffraction peak, as a function of Zr content (see inset in Fig. 1). The CZ15 mixed oxide exhibited a different pattern characterized by the presence of both, the fluorite-like CeO_2 and the monoclinic ZrO_2 (JCPDS 37-1484) structures. As indicated for the CZ50 oxide, we cannot rule out either in this case the presence of the tetragonal structure. The characterization by HREM confirmed the formation of a Ce–Zr–O solid solution in the cases of CZ80, CZ68 and CZ50 oxides. As an example, Fig. 2A shows a typical image obtained for the CZ68 sample. The inset in this figure shows the digital diffraction pattern (DDP) corresponding to the selected particle. This pattern could be indexed to the cubic structure along the [1,1,0] zone axis or, alternatively, to a tetragonal structure along the [1,1,1] or even the [0,1,0] or [1,0,0], in which some spots are not seen (Fig. SI1). According to dynamic simulations, the additional spots of the tetragonal structure (missing in the DDP) would only gain intensity in the case of particles thicker than the ones obtained in our case. The elemental EDS analyses indicated a high compositional homogeneity. The compositions obtained by this technique (spatial resolution better than 1 nm) were close to the nominal values for CZ80, CZ68 and CZ50 mixed oxides.

Fig. 2B and C corresponds to the TEM characterization of the CZ15 sample. In addition to the presence of Ce–Zr mixed oxide (Fig. 2B), the segregation of Zr forming ZrO_2 is confirmed by the DDP shown in Fig. 2C, which can be unequivocally attributed to monoclinic ZrO_2 either in the [1,1,−1] or [1,1,1] zone axis (Fig. SI1). The compositional analysis of these particles was made by EDS. This technique confirmed the presence ZrO_2 nanoparticles with a very poor content in Ce. On the other hand, the composition of the mixed oxide was close to $Ce_{0.20}Zr_{0.80}O_2$, which is slightly enriched in cerio content compared with the nominal composition.

The reducibility of Ce–Zr oxides was investigated by means of TPR experiments, following the evolution of water under flowing H_2 (5%)/Ar as a function of temperature. The reduction profiles are shown in Fig. 3. The CZ100 sample presented the well-known profile for ceria consisting of two peaks at 495 and 890 °C, attributed to surface and bulk reduction, respectively [20,21]. In contrast to the TPR profile for pure ceria, CeZr samples showed essentially a main single broad reduction feature centred around 560–570 °C. An additional reduction contribution is also observed at moderate temperature (350–420 °C) for Zr-rich oxides, being more evident in the case of CZ15. The analysis of these profiles suggests that, in contrast to pure ceria, the surface and bulk reduction processes in CeZr oxides occur concurrently. This fact is generally explained in terms of a higher mobility of the lattice oxygen, as a consequence of the vacancies or structural defects created by the incorporation of Zr into the ceria fluorite structure [22].

Another important aspect related to redox properties is the maximum degree of reduction achieved by the oxides. To measure this reduction degree, the samples reduced in TPR experiments were submitted to reoxidation with pulses of O_2 at 427 °C. According to [23], this treatment leads to fully reoxidized samples, so the O_2 uptake can be considered as a measure of the amount of oxygen vacancies created upon reduction. Fig. 4 shows the effect of the sample composition on the oxygen uptake. We can observe that, compared to pure ceria (CZ100), the addition of Zr significantly increases the amount of oxygen vacancies created during the TPR experiments. Similar values were found for CZ50, CZ68 and CZ80 samples. For the Zr richest oxide (CZ15), the O_2 uptake dramatically decreased to 0.26 mmol g^{-1}. As indicated previously when discussing TPR results, this behaviour can be interpreted in terms of a higher mobility of oxygen atoms as a consequence of the introduction of Zr in the ceria lattice [9,17].

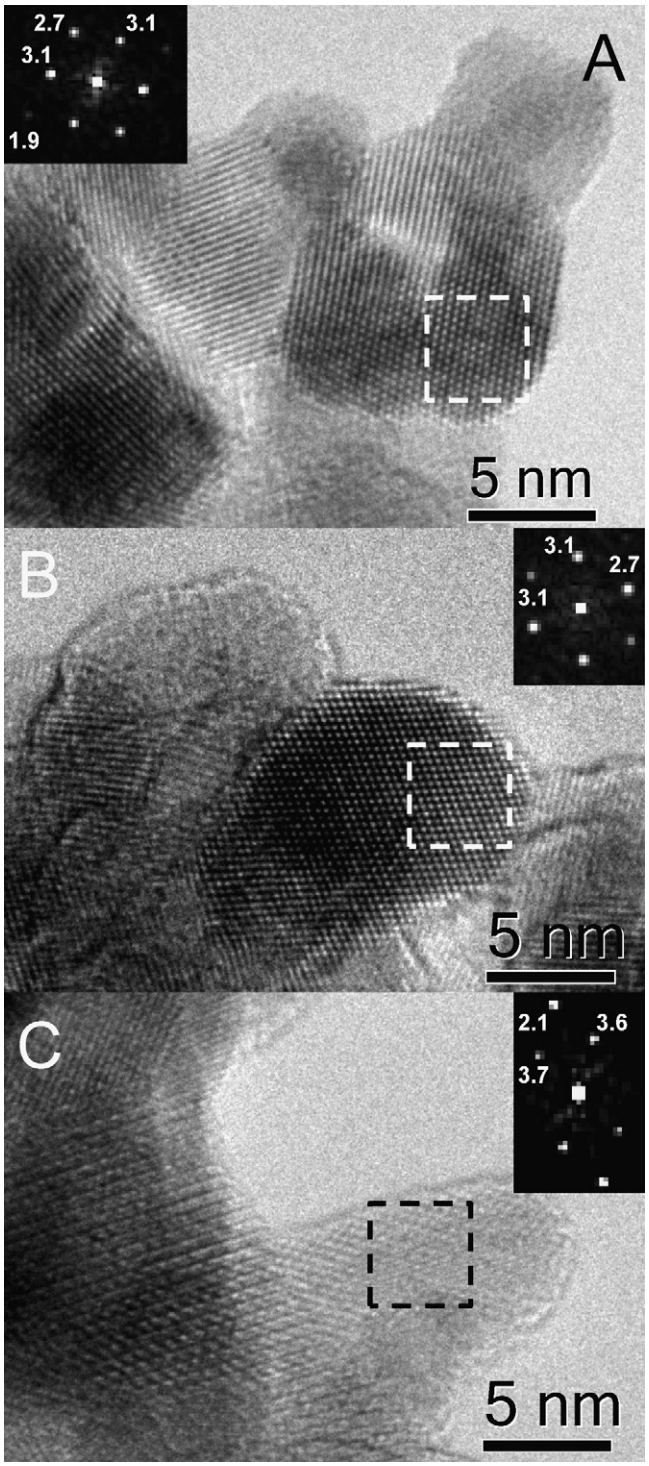

Fig. 2. TEM images of fresh samples: (A) CZ68 and CZ15 (B and C). The included DDP corresponds to the marked area.

Fig. 4 also includes the percentage of Ce^{4+} reduced to Ce^{3+} during the TPR experiment, calculated considering the O_2 uptake and the total amount of cerium in each sample. We can observe that the percentage of cerium reduced also increases with the Zr content, the sample CZ15 exhibiting the highest value of $\%Ce^{+3}$, close to 100%.

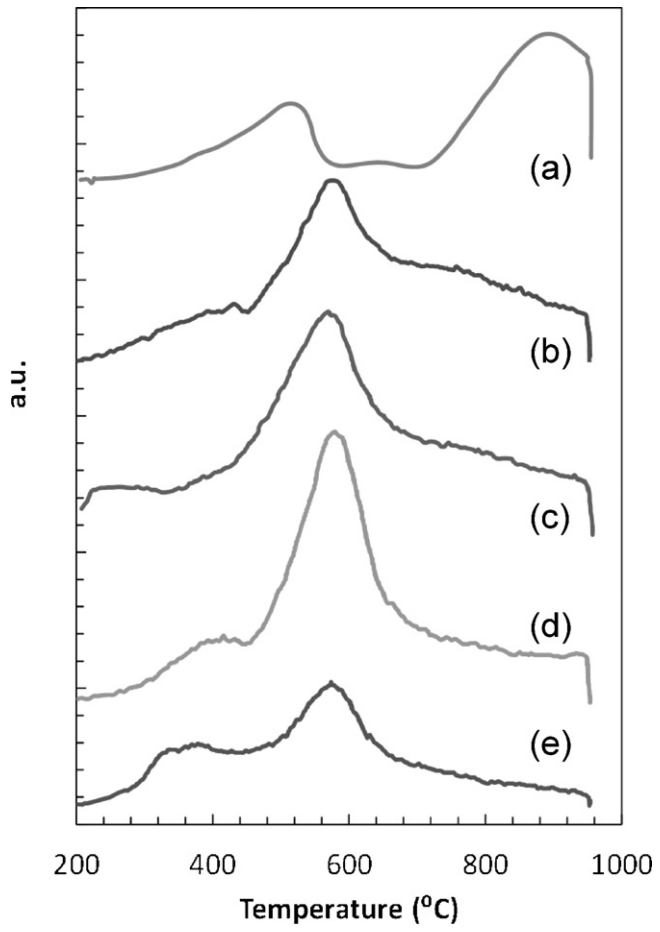

Fig. 3. TPR profiles of samples CZ100 (a) CZ80 (b), CZ68 (c), CZ50 (d) and CZ15 (e).

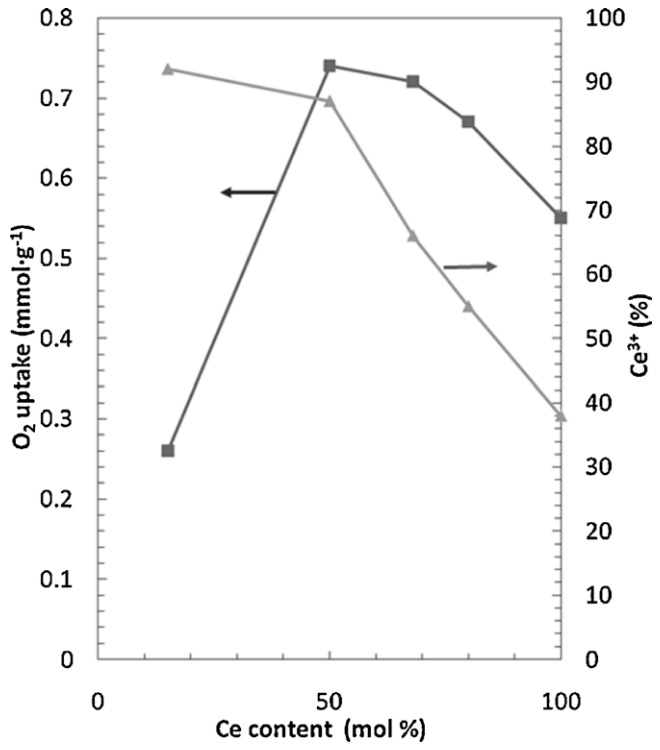

Fig. 4. Oxygen uptake and ceria reduction degree after TPR experiments as a function of the sample composition.

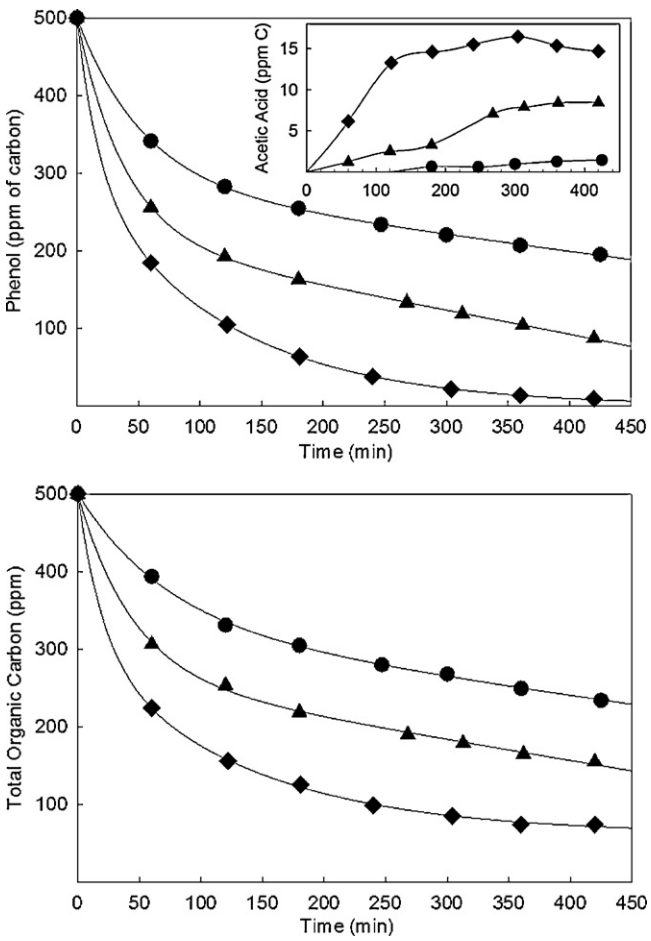

Fig. 5. Phenol concentration (top) and total organic carbon (bottom) evolution in different CWO experiments using 2.0 MPa of oxygen and 120 °C (•), 140 °C (▲) and 160 °C (♦). The evolution of acetic acid is included as inset.

However, we should also consider that the amount of cerium susceptible of been reduced obviously is minimum in the case of CZ15. Thus, and combining the results obtained in TPR and O_2 uptake experiments, we can conclude that an intermediate concentration of zirconium in the sample would be the best compromise between oxygen availability and mobility in CeZr mixed oxides. In other words, oxides with cerium contents in the range 50–70% would exhibit the highest concentration of reactive oxygen, this being the main reason for the improvement in redox properties with respect to pure CeO_2 and ZrO_2 oxides.

3.2. Catalytic tests

3.2.1. Effect of the temperature of reaction on phenol and TOC conversion

Fig. 5 shows the evolution of the TOC and phenol concentration in CWO of phenol experiments at different temperatures over the CZ68 catalyst. We observe that, as expected, the temperature greatly affects the activity for phenol conversion and TOC abatement. The initial amount of phenol in these experiments (500 ppm of C) was completely converted operating at 160 °C during 6 h. After this time, the phenol conversion obtained at 120 °C was only of 60%. As observed in Fig. 5, the values of TOC concentration were always higher than those obtained for phenol concentration, thus indicating the presence of refractory intermediate compounds, basically acetic acid, formed during the reaction. The inset in Fig. 5 shows the evolution of acetic acid concentration. We can observe that acetic acid is formed from the very initial stage of the reaction, and its

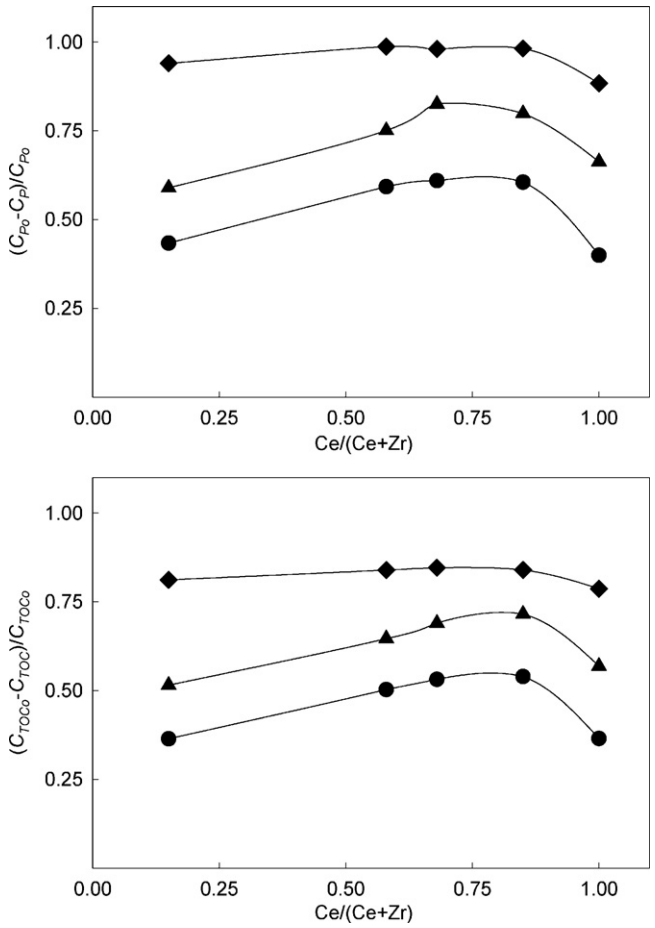

Fig. 6. Phenol (top) and total organic carbon (bottom) removal after a reaction time of 420 min as a function of the catalyst composition using 2.0 MPa of oxygen and 120 °C (•), 140 °C (▲) and 160 °C (♦).

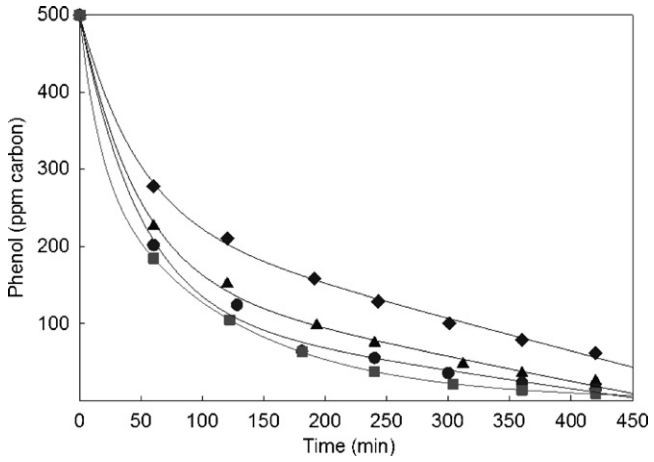

Fig. 7. Phenol concentration evolution using the CZ68 sample at 160 °C and 2.0 (■), 1.5 (•), 1.0 (▲) and 0.5 (♦) MPa of oxygen (total pressure 3.5 MPa).

concentration increased up to a maximum and stable value. As a consequence of the acetic acid formation, the pH decreased up to 4–3. The concentration of acetic acid at the end of the run was almost negligible in the case of the assay carried out at 120 °C, but significantly important at higher temperatures. In other words, the amount of residual acetic acid increased with phenol (or TOC) conversion. To better evaluate the capacity of Ce/Zr mixed oxides for acetic acid removal, several CWO runs of this compound (initial concentration = 1250 ppm) were performed in the same range of temperatures used for phenol oxidation. Conversions were always lower than 3%, thus corroborating the reduced capacity of Ce/Zr for the oxidation of this rather refractory compound. Similar results were obtained by Trovarelli et al. by investigating the wet oxidation of acetic acid on a $Ce_{0.8}Zr_{0.2}O_2$ at 190 °C [24]. The authors found that, even at this temperature, only 27% of the initial compound was converted after 7 h of reaction.

3.2.2. *Effect of the catalyst composition on phenol and TOC conversion*

The effect of the catalyst composition in the CWO of phenol is presented in Fig. 6. Although all the catalysts were active for the reaction, the activity shown depended on the Ce/Zr molar ratio of the oxides. We observed that in terms of both, phenol (Fig. 6A) and TOC (Fig. 6B) removal, the better performances were obtained with CZ50, CZ68 and CZ80 catalysts. The differences with respect to CZ15 (the Zr-richest composition) and CZ100 (pure ceria) were especially evident at the lowest reaction temperature. It is important to note the very high conversion values obtained at 160 °C (close to 100%), which prevent from establishing differences between catalysts at this temperature. The enhancement of the oxidation activity for intermediate compositions could be explained by the higher reducibility exhibited by these oxides. In effect, as deduced from structural and redox characterization, the replacement of Ce^{4+} by the smaller Zr^{4+} ions provoked a structural modification of the original fluorite-like structure through a defective cubic and/or tetragonal solid solution in which oxygen ion mobility is enhanced, as evidenciated by the lower temperature onset for oxygen removal (as H_2O) in TPR experiments and the higher O_2 uptake values measured on these samples. In this sense, it is worth of noting the similitude in shape between the graphics corresponding to conversions at low temperature in Fig. 6, and that reporting for O_2 uptake experiments in Fig. 4. In the case of the CZ15 oxide, the observed phenol (and TOC) conversion values can be explained considering that the low amount of oxygen available in this Ce-poorest oxide is more easily released (Fig. 3). The CWO process is carried out at relatively soft operation conditions and for this reason the availability of oxygen at low temperature plays such as an important role.

3.2.3. *Effect of the oxygen partial pressure on phenol and TOC conversion*

The effect of the partial pressure of oxygen on the conversion of phenol was evaluated in the range 0.5–2.0 MPa. These experiments were performed over the CZ68 catalyst at 160 °C. The phenol removal curves (Fig. 7) are characterized by a fast reduction during the first 2–3 h of reaction followed by a linear dependence of phenol concentration with time, this latter being much more evident in the case of the experiment performed at 0.5 MPa. As deduced from this figure, the influence of the partial pressure of oxygen on the final conversion (after 7 h of reaction) is almost negligible for values higher than 0.5 MPa.

3.2.4. *Effect of the phenol/catalyst ratio on phenol and TOC conversion*

The effect of the phenol/catalyst ratio was investigated in two series of experiments using the CZ68 catalyst at 160 °C and oxygen partial pressure of 2.0 MPa. In the first series, the initial phenol concentration varied from 250 to 3900 ppm. The amount of catalyst was always 1 g (3.85 g/l). In the second series, three experiments were done with a catalyst load of 1.92, 3.85 and 5.77 g/l, respectively. The initial concentration of phenol was set to 500 ppm. The results corresponding to the first series of experiments are presented in Fig. 8. The phenol is almost completely converted when using concentrations of this contaminant below 1000 ppm. When total conversion was not achieved (concentration higher

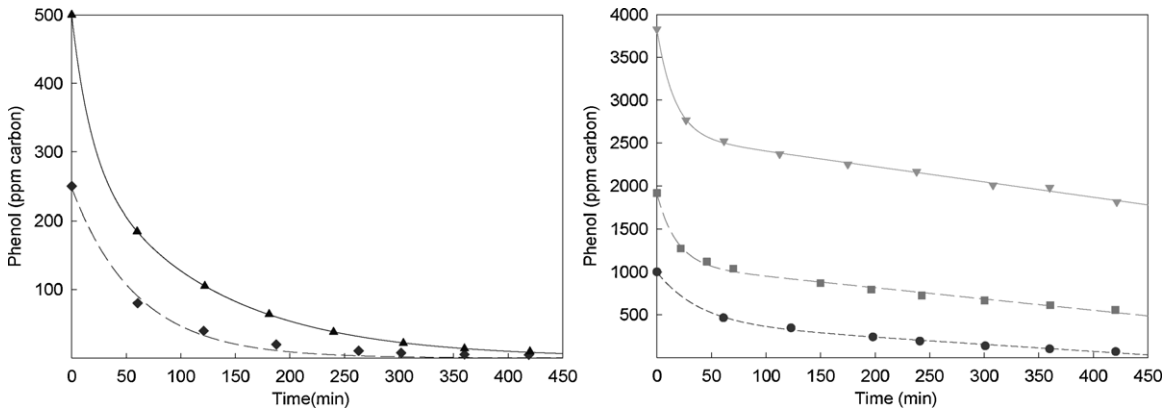

Fig. 8. Phenol evolution in CWO runs over the CZ68 catalyst as a function of the initial phenol concentration (250 (♦), 500 (▲), 1000 (•), 1900 (■) and 3800 (▼)). Reaction conditions: T^{a} = 160 °C, P_{O_2} = 2.0 MPa, catalyst loading = 1 g.

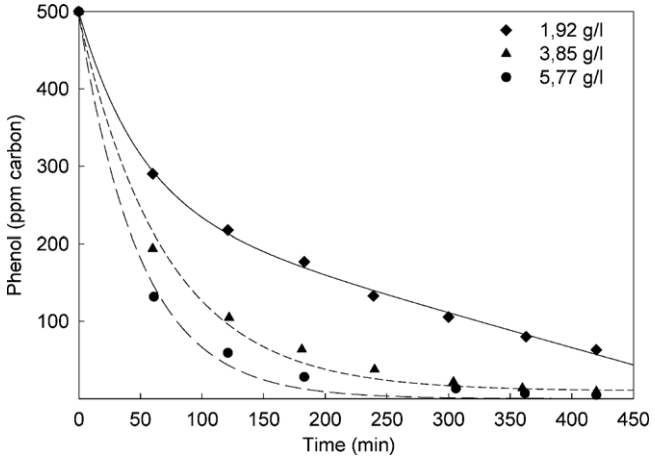

Fig. 9. Phenol evolution in CWO runs over the CZ68 catalyst as a function of the catalyst loading (T^{a} = 160 °C, P_{O_2} = 2.0 MPa, phenol initial concentration = 500 ppm).

than 1000 ppm), a phenol evolution profile similar to the ones described in previous section was obtained. As seen in Fig. 8, these profiles are characterized by a fast slope of phenol at the beginning of the reaction followed by a linear reduction of its concentration with time. Similar profiles were obtained in terms of TOC abatement. The results obtained by varying the catalyst loading are presented in Fig. 9. Under these operating conditions, the catalyst loading did not significantly influence the maximum conversion. Only a very small improvement in initial conversion was observed when increasing the amount of catalyst from 3.85 to 5.77 g/l. In the case of the lowest catalyst loading (1.92 g/l), the rate of phenol disappearance was much lower, and also in this case, a low-sloped linear dependence of the phenol concentration with time was observed at the end of the run. According to these results, we can conclude that the linear part of the phenol conversion profile accounts for a step of the phenol oxidation mechanism that is favoured when using high phenol to catalyst loading ratio.

3.3. Characterization of the catalysts after reaction

Fig. 10 shows representative HREM images corresponding to the CZ68 oxide after the catalytic runs at 120 °C (A) and 160 °C (B). The presence of a carbonaceous layer partially covering the catalytic surface can be clearly observed after the low temperature essay (Fig. 10A). On the contrary, a clean surface was observed in the case of the run performed at 160 °C. The TEM images also indicate that the carbonaceous layers exhibit fully amorphous structure, in good accordance with the low graphitization level of the deposits formed on MnO_2–CeO_2 catalysts after CWAO reactions [25]. The analysis by means of TEM and XRD of the used catalysts indicated that no structural changes occurred during the reaction (Fig. SI2). Regarding its textural properties, only a slight decrease in surface area was observed, likely provoked by the carbonaceous deposit

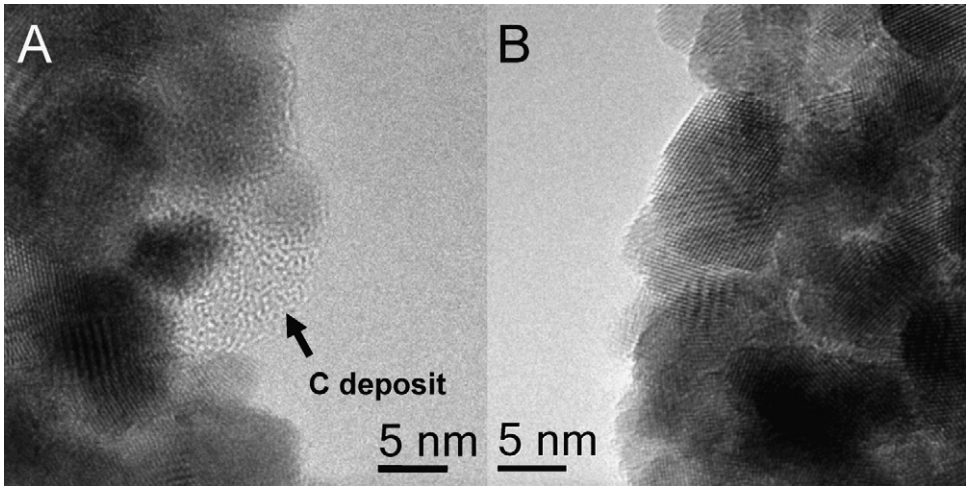

Fig. 10. TEM micrographs of the sample CZ68 after reaction at 120 °C (A) and 160 °C (B). Coke (marked) was only observed after reaction at lower temperature.

Table 2
Phenol (and TOC) conversions, selectivities to CO_2 and carbon mass balances corresponding to catalytic tests at different reaction temperature (P_{O_2} = 2.0 MPa, $[Ph]_o$ = 500 ppm).

T^q (°C)	Sample	S_{BET}[a] ($m^2\ g^{-1}$)	C_{phenol} (%)	C_{TOC} (%)	S_{CO_2} (%)	C-mass balance (%)			
						Phenol	Intermediates	C-deposit	CO_2
160	CZ100	99.6	88.4	78.8	79.6	11.6	9.6	8.5	70.3
	CZ68	97.5	98.2	85.2	84.1	1.8	13.0	2.7	82.5
	CZ15	92.2	89.6	81.2	83.8	10.4	8.4	6.1	75.1
120	CZ100	95.3	40.0	36.8	23.6	60.0	3.2	27.4	9.4
	CZ68	87.0	60.9	53.2	36.5	39.1	7.7	31.0	22.2
	CZ15	90.3	43.4	36.4	28.2	56.6	7.0	24.2	12.2

[a] Surface area of the catalysts after reaction.

Table 3
Phenol (and TOC) conversions, selectivities to CO_2 and carbon mass balances in experiments at different oxygen partial pressures ($[Ph]_o$ = 500 ppm, T^q = 160 °C, catalyst: CZ68).

P_{O_2} (MPa)	C_{phenol} (%)	C_{TOC} (%)	S_{CO_2} (%)	C-mass balance (%)			
				Phenol	Intermediates	C-deposit	CO_2
0.5	87.8	73.4	74.5	12.2	14.4	8.0	65.4
1.0	94.9	83.7	83.1	5.1	11.2	4.8	78.9
1.5	97.0	83.3	82.5	3.0	13.7	3.3	80.0
2.0	98.2	85.2	83.8	1.8	13.0	2.9	82.3

and therefore correlated with the carbon content measured after reaction (see Table 2).

The profiles of O_2 consumption and CO_2 and H_2O formation during the TPO analysis of the CZ68 catalyst, once recovered from the run at 120 °C, are shown in Fig. 11. As deduced from this figure, the carbonaceous deposit could be completely burned-off by calcination at mild temperatures (<350 °C), thus regenerating the catalytic capacity of the catalyst for the wet oxidation of phenol.

The leaching of metals was investigated by analysing the concentration of Ce and Zr in the liquid at the end of the runs. The values obtained by ICP were always below the detection limits of the technique (<0.05 ppm), thus indicating a high stability of the Ce–Zr oxide catalysts under the experimental conditions used in this work.

3.4. Carbon-mass balance and CO_2 selectivity

In the wet oxidation reaction, phenol is converted into organic intermediates, which remain in the liquid, carbonaceous deposits, adsorbed on the surface of the catalysts, and carbon dioxide. In order to establish the real capacity of Ce–Zr oxides for the mineralization of phenol, the amounts of CO_2, intermediates and carbonaceous deposits must be quantified. For this purpose, carbon mass balances were carried out at the end of the runs. The results for these balances, in terms of percentage of carbon, along with CO_2 selectivities, expressed as the fraction of the total converted carbon that is mineralized into CO_2, are reported in Tables 2–4 for the set of catalytic tests previously commented. Phenol and TOC conversions are also included for a better analysis of the data. In our case, only acetic acid was identified as intermediate.

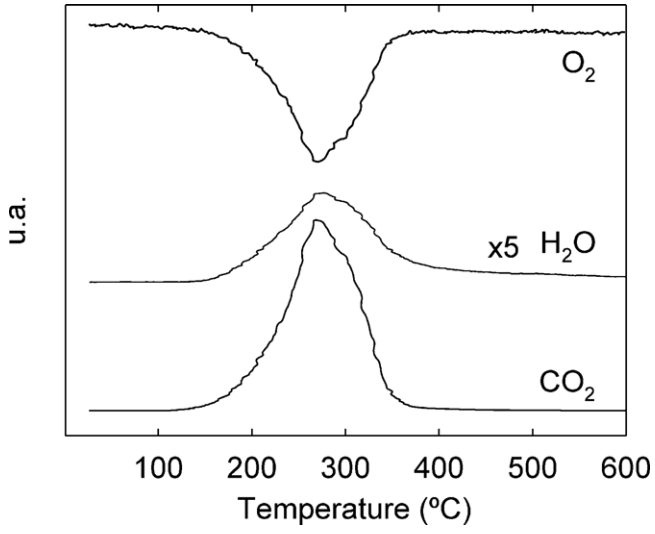

Fig. 11. Traces of O_2, H_2O and CO_2 during TPO analysis of the CZ68 catalyst after reaction at 120 °C.

In general, the carbon contents obtained for Ce–Zr oxides were similar to the ones reported by Nousir et al. [26], and significantly lower than those previously reported for other catalytic formulations also active in the wet oxidation of phenol, like Ce–Mn oxides [13,27]. Moreover, it should be pointed out that, in spite of the well-recognized ability of Ce–Mn oxides for phenol oxidation in terms of phenol or TOC conversion (100% of phenol converted at 90 °C after 4 h), they generally exhibit rather lower mineralization than Ce–Zr oxide catalysts when operating at moderate temperatures (90–140 °C).

As it can be seen in Table 2, there is a significant influence of the temperature on the CO_2 selectivity. At 160 °C, the initial phenol concentration is almost completely converted into CO_2 after 7 h (S_{CO_2} higher than 79%), and consequently the amounts of intermediates and carbonaceous deposits formed are very low. When operating at 120 °C, the selectivity to carbon dioxide is significantly reduced, basically due to the presence of a higher amount of deposit adsorbed on the catalytic surface. To have a more precise idea about the influence of the temperature on the formation of the carbonaceous deposit, additional runs at 120 °C and 160 °C were performed with the CZ68 catalyst and stopped when reaching a TOC conversion of 60% in both cases. The carbon content was double in the case of the experiment performed at 120 °C, thus confirming that, for the same conversion value, the higher the temperature, the lower the amount of deposit adsorbed on the catalyst. Regarding the influence of the catalyst composition on the mineralization of phenol, we observed that CO_2 selectivity was higher in Zr-containing samples, the highest value being obtained for the CZ68 oxide, irrespectively of the temperature of reaction. Thus, the S_{CO_2} obtained whit this oxide at 120 °C is roughly double than those obtained with CZ100 and CZ15 oxides. It is worth of noting that the CZ68 oxide also showed the higher carbon content after the run at 120 °C, thus suggesting that the formation of the carbonaceous deposits might not

Table 4
Phenol (and TOC) conversions, selectivities to CO_2 and carbon mass balances in experiments with different initial phenol concentrations (P_{O_2} = 2.0 MPa, T^{a} = 160 °C, catalyst: CZ68).

$[Ph]_o$ (ppm)	C_{phenol} (%)	C_{TOC} (%)	S_{CO_2} (%)	C-mass balance (%)				Slope[a] (ppm min^{-1})	Cc[b] (%)
				Phenol	Intermediates	C-deposit	CO_2		
250	98.2	80.6	80.4	1.8	17.6	1.6	79.0	–	0.3
500	98.2	85.2	83.8	1.8	13.0	2.9	82.3	–	0.3
1000	93.1	79.2	79.2	6.9	13.9	5.5	73.7	−0.81	1.4
1900	70.9	60.1	48.1	29.1	10.8	26.0	34.1	−1.17	11.4
3800	52.7	43.6	46.5	47.3	9.1	19.1	24.5	−1.11	15.8

[a] Obtained by least squares regression analysis of the linear parts of the curves (squares of the regressions coefficients > 0.999).
[b] Carbon content referred to the weight of catalyst.

be just considered as a deactivation process, but rather as a part of the mechanism for the total mineralization of phenol under these conditions.

The effect of the oxygen partial pressure on the mineralization of CO_2 is less important than the one previously commented for temperature or catalyst composition dependence. At 160 °C, the S_{CO_2} is close to 80% for oxygen partial pressure in the range 1–2 MPa. As indicated in Table 3, there is a slight decrease in the amount of deposit when increasing the oxygen pressure from 0.5 to 2.0 MPa.

The influence of the initial concentration of phenol is illustrated in Table 4. Conversion values are close to 100% and CO_2 selectivities higher than 70% when starting from phenol concentration up to 1000 ppm. For more concentrated solutions, both, the conversion of phenol and the mineralization to carbon dioxide decreased. The relationship between mineralization and carbonaceous deposits follows the same trend already observed when discussing the effect of the temperature or oxygen partial pressure, that is, the loss of CO_2 selectivity is basically attributable to the increase in carbon content found on the catalyst surface at the end of each run. However, in this case we should take into account the differences in phenol concentration of the starting solutions. One point to be considered when using highly concentrated solutions is the limited capacity of the catalysts to adsorb the carbonaceous products, as well as the possibility of total blockage of the catalyst surface by the deposit, which might provoke the total deactivation of the catalyst. In terms of ppm of C, the residual carbon content accumulated on the surface of the CZ68 catalyst increased with the initial phenol concentration, as expected, reaching a value of 725 ppm after the run performed with the highest phenol concentration (3800 ppm). To get more insight into the role of carbonaceous deposit on the mechanism for the wet oxidation of phenol, a series of experiments were performed to monitor the evolution of the deposit as a function of the time of reaction. The results are shown in Fig. 12. Considering the evolution of phenol conversion, also included in this figure, we may suggest that, at 120 °C, phenol is basically transformed into carbonaceous deposit in a rapid process occurring at the beginning of the reaction. Once the surface is covered, the carbon content on the catalyst remains almost constant, and the rate for phenol removal significantly decreases. The evolution of the carbon content observed in a standard catalytic test at 160 °C was rather different. The deposit is newly formed very rapidly during the first minutes of reaction but, contrary to the observed at 120 °C, it decomposed in a very fast process occurring in parallel with phenol removal. These results can be interpreted according to the reaction scheme for wet oxidation of phenol proposed in [13] and briefly depicted in Fig. 13. This scheme consists of two processes occurring consecutively in the liquid medium. Firstly, in the presence of Ce–Zr oxides, phenol molecules polymerize leading to a complex mixture of organics by-products, which are very rapidly adsorbed on the surface of the catalyst. At 160 °C, this deposit is further oxidized into CO_2. The high value of CO_2 selectivity and the low amount of deposit formed at this temperature would strongly suggest that both mechanisms, the direct phenol oxidation and the formation/oxidation of the carbonaceous deposit, were taking place. However, at the lower temperature (120 °C), the polymerization of phenol is significantly favoured with respect to its direct oxidation into intermediates or CO_2. Moreover, the rate for the oxidation of the carbonaceous material at this temperature is very low, and therefore the catalyst became apparently deactivated. Assuming this global reaction mechanism, the linear part of the profiles accounting for phenol (or TOC) removal in the less active samples, or when operating at most unfavourable conditions (low temperature and oxygen partial pressure or high phenol to catalyst ratio) could be mainly associated with the oxidation of the carbonaceous layer, and its slope used as a comparative measure of the rate for this process. We have used this approximation to investigate the activity of the CZ68 catalyst for the oxidation of the polymer as a function of the carbon content adsorbed on the surface. The results are shown in Table 4. In these experiments, the formation of the carbonaceous deposits was favoured by using highly concentrated phenol solutions. As it can be seen in this table, the catalysts is still active for the oxidation of

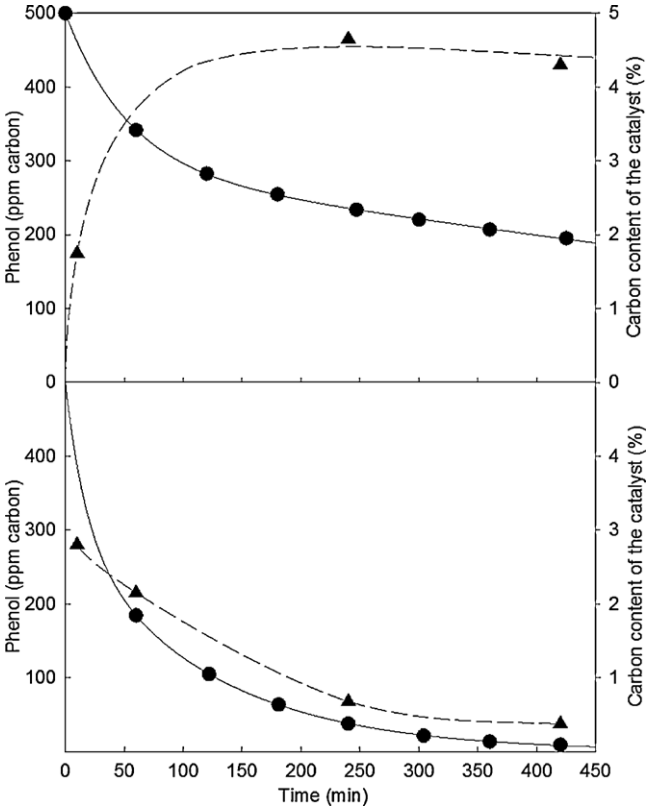

Fig. 12. Evolution of phenol (•) and coke (▲) concentration operating at 2.0 MPa of oxygen and 120 °C (top) and 160 °C (bottom).

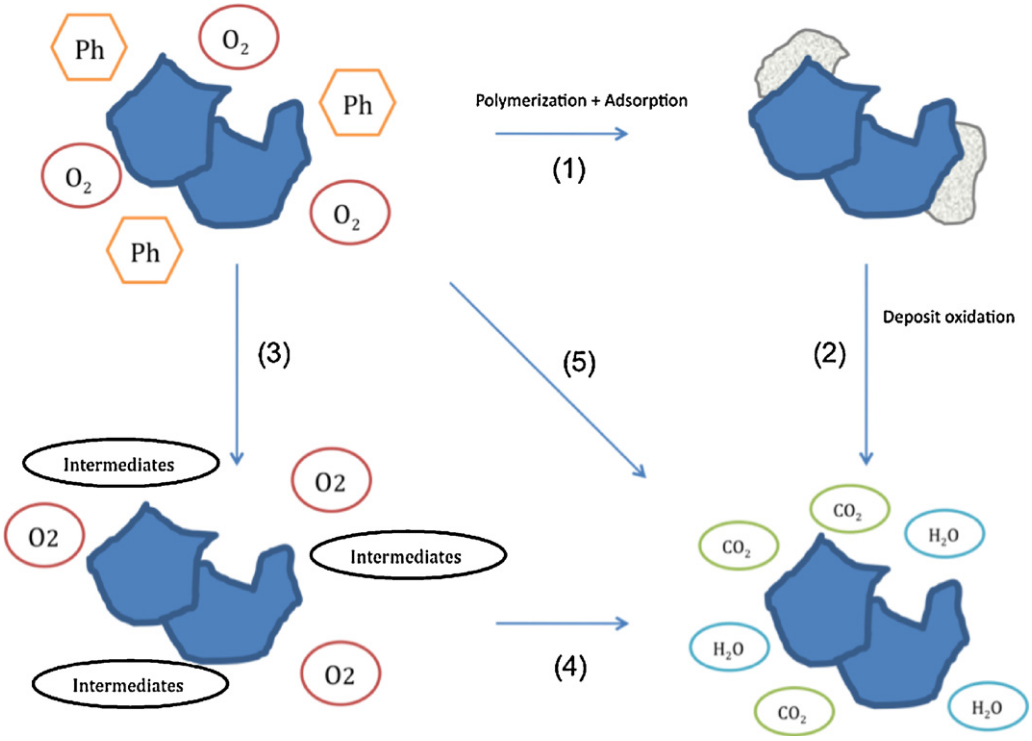

Fig. 13. Reaction scheme for wet oxidation of phenol: (1) phenol polymerization leading to a complex coke formation, (2) coke combustion on the catalyst surface, (3) partial phenol oxidation into soluble intermediates, (4) total intermediates oxidation, and (5) direct mineralization.

the deposit even when the amount of such deposits is as high as 15.8% in weight of catalyst, the rate for this process being almost constant for carbon contents higher than 11%.

4. Conclusions

The covering of the Ce–Zr catalytic particles by carbonaceous deposits, frequently associated with the total deactivation of the system, can be considered as a preliminary step of the mechanism for the CWO of phenol. The oxidation of this deposit, necessary for the desired mineralization of phenol, is favoured by employing Ce–Zr molar compositions close to 50%, at reaction temperatures above 160 °C and oxygen partial pressures higher than 0.5 MPa. The rate for this oxidation step can be deduced from the slope of the linear part of the conversion profiles as a function of time. The residual deposit remaining on the catalysts surface at the end of the run can be easily removed by calcination at 350 °C, thus regenerating the capacity of the catalysts for phenol (and TOC) removal.

Acknowledgments

Authors thank financial support from the Ministry of Science and Innovation of Spain/FEDER Program of the EU (Project: MAT2008/00889NAN and CTQ2005-02147) and the Junta de Andalucía (Proj. Ref. FQM-3994). X. Chen acknowledges the Ramón y Cajal program from Spanish Ministry of Science and Innovation. Electron microscopy data were obtained at SCCYT University of Cádiz.

Appendix A. Supplementary data

Supplementary data associated with this article can be found, in the online version, at doi:10.1016/j.cattod.2011.03.069.

References

[1] F. Luck, Catal. Today 53 (1999) 81.
[2] J. Levec, A. Pintar, Catal. Today 124 (3–4) (2007) 172.
[3] V.S. Mishra, V.V. Mahajani, J.B. Joshi, Ind. Eng. Chem. Res. 34 (1995) 2.
[4] A. Santos, P. Yustos, A. Quintanilla, F. García Ochoa, J.A. Casas, J.J. Rodrigues, Environ. Sci. Technol. 38 (2004) 133.
[5] PAT report: wet air oxidation comes of age, Environ. Sci. Technol. 9 (4) (1975) 300.
[6] S. Imamura, Ind. Eng. Chem. Res. 38 (1999) 1743.
[7] X. Hu, L. Lei, G. Chen, P.L. Yue, Water Res. 35 (8) (2001) 2078.
[8] S.H. Lin, S.J. Ho, J. Environ. Eng. 123 (1997) 852.
[9] A. Trovarelli (Ed.), Catalysis by Ceria and Related Materials, World Scientific – Imperial College Press, London, 2002.
[10] S. Imamura, A. Trovarelli (Eds.), Catalysis by Ceria and Related Materials, 14, Imperial College Press, 2002, p. 431.
[11] H. Chen, A. Sayari, A. Adnot, F. Larachi, Appl. Catal. B 32 (2001) 195.
[12] S.T. Hussain, A. Sayari, F. Larachi, Appl. Catal. B 34 (2001) 1.
[13] J.J. Delgado, J.A. Pθrez-Omil, J.M. RodrØguez-Izquierdo, M.A. Cauqui, Catal. Commun. 7 (9) (2006) 639.
[14] S. Bedrane, C. Descorme, D. Duprez, Catal. Today 75 (2002) 401.
[15] J.C. Hernandez, A.B. Hungria, J.A. Perez-Omil, S. Trasobares, S. Bernal, P.A. Midgley, A. Alavi, J.J. Calvino, J. Phys. Chem. C 111 (26) (2007) 9001.
[16] Adsorption, Surface Area and Porosity, Academic Press, London, 1991.
[17] H. Vidal, J. Kaspar, M. Pijolat, G. Colon, S. Bernal, A. Cord≤n, V. Perrichon, F. Fally, Appl. Catal. B: Environ. 27 (1) (2000) 49.
[18] M. Yashima, H. Arashi, M. Kakihana, M. Yoshimura, J. Am. Ceram. Soc. 77 (4) (1994) 1067.
[19] J. Kaspar, P. Fornasiero, M. Graziani, Catal. Today 50 (2) (1999) 285.
[20] H.C. Yao, Y.F.Y. Yao, J. Catal. 86 (2) (1984) 254.
[21] A. Trovarelli, F. Zamar, J. Llorca, C. Leitenburg, G. Dolcetti, J.T. Kiss, J. Catal. 169 (1997) 490.
[22] G. Balducci, J. Kaspar, P. Fornasiero, M. Graziani, M.S. Islam, J.D. Gale, J. Phys. Chem. B 101 (10) (1997) 1750.
[23] P. Fornasiero, R. Di Monte, G. Ranga Rao, J. Kaspar, S. Meriani, A. Trovarelli, M. Graziani, J. Catal. 151 (1) (1995) 168.
[24] C. De Leitenburg, D. Goi, A. Primavera, A. Trovarelli, G. Dolcetti, Appl. Catal. B 11 (1996) L29.
[25] S. Hamoudi, F. Larachi, A. Adnot, A. Sayari, J. Catal. 185 (1999) 333.
[26] S. Nousir, S. Keav, J. Barbier, M. Bensitel, R. Brahmi, D. Duprez, Appl. Catal. B: Environ. 84 (3–4) (2008) 723.
[27] F. Arena, G. Trunfio, J. Negro, L. Spadaro, Appl. Catal. B: Environ. 85 (1–2) (2008) 40.